Examining abnormal Silurian trilobites from the Llandovery of Australia (#76247)

First submission

Guidance from your Editor

Please submit by **7 Sep 2022** for the benefit of the authors (and your token reward) .

Structure and Criteria
Please read the 'Structure and Criteria' page for general guidance.

Raw data check
Review the raw data.

Image check
Check that figures and images have not been inappropriately manipulated.

Privacy reminder: If uploading an annotated PDF, remove identifiable information to remain anonymous.

Files
Download and review all files from the materials page.

6 Figure file(s)
1 Table file(s)
1 Raw data file(s)

Structure and Criteria

Structure your review

The review form is divided into 5 sections. Please consider these when composing your review:

1. **BASIC REPORTING**
2. **EXPERIMENTAL DESIGN**
3. **VALIDITY OF THE FINDINGS**
4. General comments
5. Confidential notes to the editor

You can also annotate this PDF and upload it as part of your review

When ready submit online.

Editorial Criteria

Use these criteria points to structure your review. The full detailed editorial criteria is on your guidance page.

BASIC REPORTING

- Clear, unambiguous, professional English language used throughout.
- Intro & background to show context. Literature well referenced & relevant.
- Structure conforms to PeerJ standards, discipline norm, or improved for clarity.
- Figures are relevant, high quality, well labelled & described.
- Raw data supplied (see PeerJ policy).

EXPERIMENTAL DESIGN

- Original primary research within Scope of the journal.
- Research question well defined, relevant & meaningful. It is stated how the research fills an identified knowledge gap.
- Rigorous investigation performed to a high technical & ethical standard.
- Methods described with sufficient detail & information to replicate.

VALIDITY OF THE FINDINGS

- Impact and novelty not assessed. *Meaningful* replication encouraged where rationale & benefit to literature is clearly stated.
- All underlying data have been provided; they are robust, statistically sound, & controlled.
- Conclusions are well stated, linked to original research question & limited to supporting results.

Standout reviewing tips

The best reviewers use these techniques

Tip	*Example*
Support criticisms with evidence from the text or from other sources	*Smith et al (J of Methodology, 2005, V3, pp 123) have shown that the analysis you use in Lines 241-250 is not the most appropriate for this situation. Please explain why you used this method.*
Give specific suggestions on how to improve the manuscript	*Your introduction needs more detail. I suggest that you improve the description at lines 57- 86 to provide more justification for your study (specifically, you should expand upon the knowledge gap being filled).*
Comment on language and grammar issues	*The English language should be improved to ensure that an international audience can clearly understand your text. Some examples where the language could be improved include lines 23, 77, 121, 128 – the current phrasing makes comprehension difficult. I suggest you have a colleague who is proficient in English and familiar with the subject matter review your manuscript, or contact a professional editing service.*
Organize by importance of the issues, and number your points	*1. Your most important issue* *2. The next most important item* *3. …* *4. The least important points*
Please provide constructive criticism, and avoid personal opinions	*I thank you for providing the raw data, however your supplemental files need more descriptive metadata identifiers to be useful to future readers. Although your results are compelling, the data analysis should be improved in the following ways: AA, BB, CC*
Comment on strengths (as well as weaknesses) of the manuscript	*I commend the authors for their extensive data set, compiled over many years of detailed fieldwork. In addition, the manuscript is clearly written in professional, unambiguous language. If there is a weakness, it is in the statistical analysis (as I have noted above) which should be improved upon before Acceptance.*

Examining abnormal Silurian trilobites from the Llandovery of Australia

Russell D C Bicknell [Corresp., 1], **Patrick M Smith** [2, 3]

[1] Palaeoscience Research Centre, School of Environmental and Rural Science, University of New England, Armidale, New South Wales, Australia

[2] Department of Biological Sciences, Macquarie University, Sydney, New South Wales, Australia

[3] Palaeontology Department, Australian Museum Research Institute, Sydney, New South Wales, Australia

Corresponding Author: Russell D C Bicknell
Email address: rdcbicknell@gmail.com

Abnormal trilobites present information on how arthropods with fully biomineralised exoskeletons recovered from injuries, genetic malfunctions, and pathologies. Records of abnormal Silurian trilobites in particular show specimens with teratologies and a limited record of injuries. Here we extend the record of abnormal Silurian trilobites by presenting seven new abnormal specimens of *Odontopleura* (*Sinespinaspis*) *markhami* from the early Silurian (Llandovery, Telychian) Cotton Formation, New South Wales. We use these specimens as new examples of asymmetric distribution of thoracic nodes that are considered teratological morphologies. These nodes likely reflect genetic complications, resulting in morphologies that would unlikely have aided the population. In considering records of malformed Silurian trilobites more broadly, we propose that only the largest forms were prey at this time. This illustrates a marked change in the trophic level for trilobites when compared with the early and middle Palaeozoic ecosystems.

Examining abnormal Silurian trilobites from the Llandovery of Australia

Russell D. C. Bicknell[1,*] and Patrick M. Smith[2,3]

[1] Palaeoscience Research Centre, School of Environmental and Rural Science, University of New England, Armidale, New South Wales, 2351, Australia.

[2] Palaeontology Department, Australian Museum Research Institute, Sydney, New South Wales, 2010, Australia.

[3] Department of Biological Sciences, Macquarie University, Sydney, New South Wales, 2109, Australia.

[*] Corresponding author: rdcbicknell@gmail.com

ORCiD: RDCB: 0000-0001-8541-9035

Abstract

Abnormal trilobites present information on how arthropods with fully biomineralised exoskeletons recovered from injuries, genetic malfunctions, and pathologies. Records of abnormal Silurian trilobites in particular show specimens with teratologies and a limited record of injuries. Here we extend the record of abnormal Silurian trilobites by presenting seven new abnormal specimens of *Odontopleura* (*Sinespinaspis*) *markhami* from the early Silurian (Llandovery, Telychian) Cotton Formation, New South Wales. We use these specimens as new examples of asymmetric distribution of thoracic nodes that are considered teratological morphologies. These nodes likely reflect genetic complications, resulting in morphologies that would unlikely have aided the population. In considering records of malformed Silurian trilobites more broadly, we propose that only the largest forms were prey at this time. This illustrates a marked change in the trophic level for trilobites when compared with the early and middle Palaeozoic ecosystems.

Keywords: Abnormalities, trilobites, Paleozoic, teratology, Silurian, *Odontopleura* (*Sinespinaspis*) *markhami*

Introduction

Abnormal extinct organisms represent invaluable insights into predator-prey interactions, genetic malfunctions, and injury recovery for fossil groups (Owen, 1985; Babcock, 1993a, 2003, 2007; Kelley et al., 2003; Huntley, 2007; Klompmaker & Boxshall, 2015; Leung, 2017). Due to the palaeobiological importance of these specimens, abnormalities have been documented in many fossil groups (Klompmaker et al., 2019). Euarthropods, in particular, have been documented showing injuries (Owen, 1985; Bicknell & Paterson, 2018), pathologies (Lochman, 1941; Šnajdr, 1978b), and teratologies (Pocock, 1974; Lee et al., 2001; Bicknell & Smith, 2021). While abnormalities are known from arachnids (Mitov et al., 2021), crustaceans (Bishop, 1972; Klompmaker et al., 2013, 2014), and horseshoe crabs (Bicknell et al., 2018), the most well documented abnormal euarthropods are trilobites (Šnajdr, 1978a; Owen, 1983, 1985; Babcock, 1993a, 2003; Fatka et al., 2015, 2021; Bicknell et al., 2019; Bicknell & Holland, 2020; Zong, 2021). This detailed record of trilobite abnormalities reflects the biomineralised dorsal exoskeleton exhibited by the group. This morphology increases the preservational protentional of specimens and readily permits the record of abnormal structures. Trilobites are, therefore, an ideal group for understanding how a wholly extinct clade of euarthropods experienced and recovered from abnormalities.

Most documented abnormal trilobite specimens are from the Cambrian Period (Owen, 1985; Babcock, 1993a, 2003; Pates et al., 2017; Pates & Bicknell, 2019; Bicknell & Pates, 2020; Zong, 2021). These specimens commonly record failed predation attempts (Rudkin, 1979; Babcock, 1993a; Bicknell & Paterson, 2018), and show limited evidence for genetic or teratological complications (see Bergström & Levi-Setti, 1978; Bicknell et al., 2022a). By contrast, the record of abnormal, post-Cambrian trilobites show developmental malformations,

teratologies, and pathologies, with fewer injuries derived from predation (Owen, 1985; Rudkin, 1985; Zong, 2021; Bicknell et al., 2022b). Silurian-aged deposits in particular preserved a diverse array of abnormal taxa across at least ten families (Table 1). These abnormalities primarily reflect developmental malfunctions (Šnajdr, 1981a; Bicknell & Smith, 2021), injuries and abnormal recovery from moulting (Šnajdr, 1981a), with rarer evidence for failed attacks (Chinnici & Smith, 2015; Bicknell et al., 2019) and accidental trauma (Rudkin, 1985). These specimens also present insight into how the ornate, often iso- to macropygous, Silurian taxa recovered from moulting and developmental complications. Historically, most abnormal Silurian trilobites are reported from deposits in the Czech Republic (Přibyl & Vaněk, 1962, 1986; Šnajdr, 1976, 1978a, b, 1979, 1980, 1981a, b), Sweden (Ramsköld, 1983, 1984; Owen, 1985; Ramsköld et al., 1994), and the USA (Campbell, 1967; Whittington & Campbell, 1967; Holloway, 1980; Rudkin, 1985; Whiteley et al., 2002; Chinnici & Smith, 2015; Bicknell et al., 2019). However, more recent records of abnormal Silurian trilobites from Australia (Bicknell & Smith, 2021) and China (Zong et al., 2017; Zong, 2021) suggest a more Gondwanan presence. To expand the limited record of abnormal Silurian trilobites from Gondwana, we considered the trilobite-rich Cotton Formation, central New South Wales (NSW) and illustrate new examples of abnormal odontopleurids (Edgecombe & Sherwin, 2001; Rickards et al., 2009).

Methods

Trilobite specimens from the Cotton Formation housed within the Australian Museum (AM F), Sydney, NSW, Australia were examined under a microscope. Seven abnormal *Odontopleura* (*Sinespinaspis*) *markhami* Edgecombe & Sherwin, 2001 specimens were identified. These specimens were dyed black with ink, coated in magnesium oxide, and photographed under low

74 angle LED light with a Canon EOS 5DS. Images were stacked using Helicon Focus 7 (Helicon
75 Soft Limited) stacking software.

76 A dataset of linear measurements was collated to determine where abnormal *Odontopleura*
77 (*Sinespinaspis*) *markhami* specimens are located relative to standard individuals in bivariate
78 space. Measurements of the cranidial length, glabellar width, and combined thorax and pygidium
79 length were taken from 46 specimens in the AM F collection (Figure 2). The dataset was
80 collated from the photographing specimens and measured using ImageJ (Schneider et al., 2012)
81 (Supplemental Data 1). Measurements were natural-log normalised and plotted, points were
82 colour coded for presence or absence of abnormalities.

83 **Geological context**

84 The material reported herein comes from "Cotton Hill Quarry", at approximately 33°18'44.0"S
85 147°56'00.9"E, on the western limb of the Forbes Anticline within the Cotton Formation. The
86 geological context of this site was discussed in vast detail by Edgecombe & Sherwin (2001, p
87 87–90). Hence, only a summary is provided here. Generally, the formation outcrops poorly,
88 appearing only as low rubbly hills in the Forbes region. Occasionally it is exposed in road and
89 rail cuttings, as well as locally in gravel quarries. The Cotton Formation at "Cotton Hill Quarry"
90 consists of well-bedded, thinly to moderately laminated siltstone which readily splits along the
91 bedding plane. The outcrop varies considerably in colour, mostly being an off-white to light
92 brownish yellow. However, in limited patches, it is deep orange to purple, often associated with
93 large Liesegang rings. The floor of the quarry reveals that the original, unweathered rock is
94 actually a darker grey colour and contains interbeds of whiter tuff which show signs of small-
95 scale slumping. The quarry walls indicate a dip at 65° to the West and a minimum thickness of
96 105 m in its upper member. Previous reports suggest the entire Cotton Formation could be much

as 1500 m in total thickness on the eastern limb of the Forbes Anticline (Sherwin, 1973), assuming a consistent dip and no cover.

Traditionally, the entire Cotton Formation was thought to range across the Ordovician – Silurian boundary (Sherwin, 1970; 1973). However, to date, only three horizons are known to contain age diagnostic graptolite faunas. The oldest of these–the "lower member"–has been assigned a possible Katian (late Ordovician) age. The "middle" and "upper members" contain fauna indicative of early and late Llandovery (Early Silurian) age respectively (Sherwin, 1974; Rickards et al., 2009). So far, there is no conclusive evidence of Hirnantian or earliest Llandovery graptolites, suggesting a significant time break between the "lower member" and the remainder two members in the formation (Percival & Glen, 2007). The material from "Cotton Hill Quarry" is derived from singular horizons within the upper most 50 m of the formation, typically the "upper member". Here the trilobites co-occur with a distinct *Spirograptus turriculatus* Zone graptolite fauna. Sherwin (1973) also noted a similar trilobite fauna proximal to the quarry, occurring about one meter above beds with the eponym of the zone. He also noted the trilobites occurred 100 m stratigraphically above a horizon with *Monograptus* cf. *sedgwicki*. This strongly supports a late Llandovery age for the "Cotton Hill Quarry" material (Edgecombe & Sherwin, 2001).

Variability in lithology of the Cotton formations' members have resulted in a variety of depositional environments suggested for the Cotton Formation (e.g. Krynen et al., 1990). The "upper member" exposed at "Cotton Hill Quarry" likely formed in a calm outer-shelf environment, below storm wave base, as evidenced by the well-laminated siltstone and the lack of disarticulated trilobites and echinoderms. The abundant planktonic graptolites and common small-eyed (or blind) trilobite taxa suggests that environment was relatively deep, limiting light

120 penetration. However, the benthic faunas (e.g. rare dendroidal graptolites, strophomenid
121 brachiopods, platyceratid gastropods and echinoderms) suggests that the bottom waters were still
122 well-oxygenated and permitted oxygen circulation.

123 **Results**

124 Abnormalities on *Odontopleura* (*Sinespinaspis*) *markhami* are minute (millimetre scale)
125 and primarily record the asymmetry of thoracic posterior pleural band spine bases. AM F126904
126 is a near complete specimen, 13.3 mm long, 10.3 mm wide (excluding genal and pleural spines)
127 with an asymmetric distribution of thoracic posterior pleural band spine bases (Figure 3A, B).
128 The seventh thoracic segment on the right pleural lobe has an additional spine base when
129 compared to the left side. AM F118762 is a moult, lacks free cheeks, is 12.2 mm long, 10.2 mm
130 wide (excluding pleural spines) with one offset spine base and one additional spine base on the
131 right pleural lobe (Figure 3C, D). The sixth thoracic segment has an offset spine base and the
132 seventh segment has an additional base. AM F115089 is a partial specimen, lacks a posterior
133 section, is 13.3 mm long, 12.0 mm wide (excluding pleural and genal spines) with an
134 asymmetrical distribution of thoracic posterior pleural band spine bases (Figure 4A, B). The first,
135 third, and fourth thoracic segments on the right pleural lobe have an additional node not observed
136 on the left lobe. AM F115081 is a partial specimen, lacking the posterior portion of the
137 exoskeleton, likely a moult, is 10.8 mm long, 7.0 mm wide (excluding pleural spines). The
138 specimen has an additional thoracic spine base on the left pleural lobe (Figure 4C, D). The third
139 thoracic segment has an additional base not observed on the right lobe. AM F145135 is 11.7 mm
140 long, 12.4 mm wide (excluding pleural and genal spines) with an additional thoracic spine base
141 on the right pleural lobe (Figure 4E, F). The second thoracic segment has an additional base not
142 observed on the left lobe. AM F118772 is likely a moult, lacks free cheeks, is 14.7 mm long,

12.9 mm wide (excluding pleural spines). The specimen has an abnormal base on the right pleural lobe (Figure 5A, B). The sixth thoracic segment has a thoracic spine base unaligned with the immediately anterior and posterior nodes. AM F133034 is likely a moult, lacks free cheeks, is 10.7 mm long, 9.1 mm wide (excluding pleural spines). The specimen has an asymmetrical distribution of thoracic posterior pleural band spine bases (Figure 5C, D). The sixth and eighth thoracic segments on the left pleural lobe have an additional bases not observed on the right lobe.

Considering the size distribution of *Odontopleura* (*Sinespinaspis*) *markhami* in bivariate space, four distinct clusters are noted (Figure 6). At least four holaspid developmental stages are therefore documented. The abnormal specimens are generally located within the second largest developmental stage. This may reflect either a developmental aspect signal or a lack of data from the other groups.

Discussion

Odontopleura (*Sinespinaspis*) *markhami* abnormalities represent additional thoracic spine base developments or offset of spine bases. Despite the presence of these abnormal structures, there is no evidence for exoskeletal removal, or any other damage to specimens. Therefore, abnormal spine base development does not reflect abnormal recovery from an injury induced during moulting or from a failed attack. These must have arisen through another process. In life, odontopleurid trilobites had large spines that preserve as spine bases on internal moulds (Bruton, 1966). Additional spine bases therefore record development of spines that arose outside the primary spine sequences. Such additional spines may have resulted in more effective defence against possible predators. However, the Cotton Formation biota show few predators (Edgecombe & Sherwin, 2001). Furthermore, the spines would not have resulted in an increased reproductive fitness as thoracic spinosity is unlikely to be a sexually selected morphology, unlike

cephalic spines (Knell & Fortey, 2005; Knell et al., 2013). Given these conditions, it seems that the additional nodes record teratological developments through genetic malfunctions and were likely unbeneficial for individuals.

The distribution of *Odontopleura* (*Sinespinaspis*) *markhami* specimens in bivariate space illustrates that most abnormal specimens are located within the second largest recorded developmental stage. This bias may reflect limited sampling from other size groups. As such, the presence of abnormal specimens in all developmental stages cannot be discounted. However, within the sampled population, it is possible that abnormalities may have become somewhat fixed in the larger specimens. *Odontopleura* (*Sinespinaspis*) *markhami* may therefore have developed abnormal spines during later growth stages.

Most examples of Silurian abnormalities (Table 1) likely record developmental complications and teratological recovery from substandard moulting (Bicknell & Smith, 2021), with rare examples of pathologies (De Baets et al., 2021). However, for the larger Silurian trilobites, such as *Arctinurus boltoni*, *Calymene niagarensis*, and *Dalmanites limulurus* from the Wenlock (Sheinwoodian) Rochester Formation, abnormalities include the removal of large exoskeletal sections (Babcock, 1993b; Whiteley et al., 2002; Chinnici & Smith, 2015; Bicknell et al., 2019). These records failed predation, as opposed to moulting complications (Chinnici & Smith, 2015; Bicknell et al., 2019), especially as these taxa lack elongated pleural spines that would have complicated moulting (Conway Morris & Jenkins, 1985; Bicknell & Pates, 2020). The size of the species, therefore, plays a fundamental role in whether trilobite groups are targeted for predation. Indeed, Cambrian trilobites represented some of the largest prey items in the period and likely had been targeted as food items (Bergström & Levi-Setti, 1978; Holmes et al., 2020; Bicknell et al., 2022a). The same is applicable for large, injured Ordovician species

(Bicknell et al., 2022b, c). However, by the Silurian, other prey items (such as eurypterids) have been preferred and only in select paleoecosystems were larger trilobite taxa subject to higher predation pressure.

Acknowledgements

This research was funded by a University of New England Postdoctoral Fellowship (to R.D.C.B.), a Karl Hirsch Memorial Grant (to R.D.C.B.), and an Australian Museum AMF/AMRI Visiting Research Fellowship (to R.D.C.B.). We thank Stephen Pates for discussions on earlier versions of the paper.

References

Angelin NP. **1854**. *Palaeontologica Scandinavica. Pars 1. Crustacea Formationis Transitionis. Fasc 2*. Leipzig: T.O. Weigel.

Babcock LE. **1993a**. Trilobite malformations and the fossil record of behavioral asymmetry. *Journal of Paleontology* **67 (2)**: 217–229.

Babcock LE. **1993b**. The right and the sinister. *Natural History* **102 (7)**: 32–39.

Babcock LE. **2003**. Trilobites in Paleozoic predator-prey systems, and their role in reorganization of early Paleozoic ecosystems. In: Kelley P, Kowalewski M, and Hansen TA, eds. *Predator-Prey interactions in the Fossil Record*: Springer, New York, 55–92.

Babcock LE. **2007**. Role of malformations in elucidating trilobite paleobiology: a historical synthesis. In: Mikulic DG, Landing E, and Kluessendorf J, eds. *Fabulous Fossils–300 Years of Worldwide Research on Trilobites*. New York: University of the State of New York, State Education Dept., New York State Museum, 3–19.

Barrande J. **1846**. *Notice Préliminaire sur le systême Silurien et les Trilobites de Bohême*. Leipzig: Hirschfeld.

Bergström J, Levi-Setti R. **1978**. Phenotypic variation in the Middle Cambrian trilobite *Paradoxides davidis* Salter at Manuels, SE Newfoundland. *Geologica et Palaeontologica* **12**: 1–40.

Bicknell RDC, Paterson JR. **2018**. Reappraising the early evidence of durophagy and drilling predation in the fossil record: implications for escalation and the Cambrian Explosion. *Biological Reviews* **93 (2)**: 754–784.

Bicknell RDC, Pates S, Botton ML. **2018**. Abnormal xiphosurids, with possible application to Cambrian trilobites. *Palaeontologia Electronica* **21 (2)**: 1–17.

Bicknell RDC, Paterson JR, Hopkins MJ. **2019**. A trilobite cluster from the Silurian Rochester Shale of New York: predation patterns and possible defensive behavior. *American Museum Novitates* **39 (3937)**: 1–16.

Bicknell RDC, Holland B. **2020**. Injured trilobites within a collection of dinosaurs: Using the Royal Tyrrell Museum of Palaeontology to document Cambrian predation. *Palaeontologia Electronica* **23 (2)**: a33.

Bicknell RDC, Pates S. **2020**. Exploring abnormal Cambrian-aged trilobites in the Smithsonian collection. *PeerJ* **8**: e8453.

Bicknell RDC, Smith PM. **2021**. Teratological trilobites from the Silurian (Wenlock and Ludlow) of Australia. *The Science of Nature* **108**: 25.

Bicknell RDC, Holmes JD, Pates S, García-Bellido DC, Paterson JR. **2022a**. Cambrian carnage: trilobite predator-prey interactions in the Emu Bay Shale of South Australia. *Palaeogeography, Palaeoclimatology, Palaeoecology* **591**: 110877.

Bicknell RDC, Smith PM, Bruthansová J, Holland B. **2022b**. Malformed trilobites from the Ordovician and Devonian. *PalZ* **96**: 1–10.

Bicknell RDC, Smith PM, Howells TF, Foster JR. **2022c**. New records of injured Cambrian and Ordovician trilobites. *Journal of Paleontology* **96:** 921–929

Bigsby JJ. **1825**. Description of a new species of trilobite. *Journal of the Academy of Natural Sciences, Philadelphia* **4**: 365–368.

Bishop GA. **1972**. Crab bitten by a fish from the upper Cretaceous Pierre Shale of South Dakota. *Geological Society of America Bulletin* **83 (12)**: 3823–3826.

Bruton DL. **1966**. *The trilobite family Odontopleuridae*: University of Leicester (United Kingdom).

Campbell KSW. **1967**. Trilobites of the Henryhouse Formation (Silurian) in Oklahoma. *Bulletin of the Oklahoma Geological Survey* **115**: 1–68.

Chang W-T. **1974**. Silurian trilobites. *In A Handbook of the Stratigraphy and Paleontology of Southwest China.* Nanking Institute of Geology and Paleontology, Academia Sinica, 173–187.

Chinnici P, Smith K. **2015**. *The Silurian Experience.* Primitive Worlds, Rochester, NY.

Chlupáč I. **1971**. Some trilobites from the Silurian/Devonian boundary beds of Czechoslovakia. *Palaeontology* **14 (1)**: 159–177.

Conrad TA. **1842**. Observations on the Silurian and Devonian systems of the United States, with descriptions of new organic remains. *Journal of the Academy of Natural Sciences of Philadelphia* **8**: 228–280.

Conway Morris S, Jenkins RJF. **1985**. Healed injuries in early Cambrian trilobites from South Australia. *Alcheringa* **9 (3)**: 167–177.

De Baets K, Budil P, Fatka O, Geyer G. **2021**. Trilobites as hosts for parasites: From paleopathologies to etiologies. In: De Baets K, and Huntley JW, eds. *The Evolution and Fossil Record of Parasitism: Coevolution and Paleoparasitological Techniques*. Cham: Springer International Publishing, 173–201.

Edgecombe GD, Sherwin L. **2001**. Early Silurian (Llandovery) trilobites from the Cotton Formation, near Forbes, New South Wales, Australia. *Alcheringa* **25 (1)**: 87–105.

Emmrich HF. 1839. De trilobitis. Friedrich-Wilhelm Universität.

Emmrich HF. **1844**. *Zur Naturgeschichte der Trilobiten*. Meiningem: Programm Realschule Meiningen.

Esmark M. **1833**. Om nogle nye Arter af Trilobiter. *Nytt Magasin for Naturvidenskap* **11**: 268–270, pl. 267.

Etheridge R, Mitchell J. **1869**. The Silurian trilobites of New South Wales, with references to those of other parts of Australia. Part 4. The Odontopleuridae. *Proceedings of the Linnean Society of New South Wales* **21**: 694–721.

Fatka O, Budil P, Grigar L. **2015**. A unique case of healed injury in a Cambrian trilobite. *Annales de Paléontologie* **101 (4)**: 295–299.

Fatka O, Budil P, Zicha O. **2021**. Exoskeletal and eye repair in *Dalmanitina socialis* (Trilobita): An example of blastemal regeneration in the Ordovician? *International Journal of Paleopathology* **34**: 113–121.

Green J. **1832**. *A monograph of the trilobites of North America: with coloured models of the species*. Philadelphia: J. Brano.

Hall J. **1843**. *Geology of New York. Part 4, comprising the survey of the fourth geological district*. Albany.

Hawle I, Corda AJ. **1847**. Prodrom einer Monographie der böhmischen Trilobiten. *Abhandlungen der Königlichen Böhmischen Gesellschaft der Wissenschaften,* **5 (5)**: 1–176.

Holloway DJ. **1980**. Middle Silurian trilobites from Arkansas and Oklahoma, U.S.A. Part I. *Palaeontographica Abteilung A* **170**: 1–85, pl 81–20.

Holmes JD, Paterson JR, García-Bellido DC. **2020**. The trilobite *Redlichia* from the lower Cambrian Emu Bay Shale Konservat-Lagerstätte of South Australia: systematics, ontogeny and soft-part anatomy. *Journal of Systematic Palaeontology* **18 (4)**: 295–334.

Howells Y. **1982**. Scottish Silurian trilobites. *Monograph of the Palaeontographical Society* **135**: 1–70.

Huntley JW. **2007**. Towards establishing a modern baseline for paleopathology: trace-producing parasites in a bivalve host. *Journal of Shellfish Research* **26 (1)**: 253–259.

Kelley P, Kowalewski M, Hansen TA. **2003**. *Predator-prey interactions in the fossil record*: Springer, New York**.**

Klompmaker AA, Karasawa H, Portell RW, Fraaije RHB, Ando Y. **2013**. An overview of predation evidence found on fossil decapod crustaceans with new examples of drill holes attributed to gastropods and octopods. *Palaios* **28 (9)**: 599–613.

Klompmaker AA, Artal P, van Bakel BWM, Fraaije RHB, Jagt JWM. **2014**. Parasites in the fossil record: a Cretaceous fauna with isopod-infested decapod crustaceans, infestation patterns through time, and a new ichnotaxon. *PLoS ONE* **9 (3)**: e92551.

Klompmaker AA, Boxshall GA. **2015**. Fossil crustaceans as parasites and hosts. In: Littlewood DTJ, and De Baets K, eds. *Advances in Parasitology*: Elsevier, 233–289.

Klompmaker AA, Kelley PH, Chattopadhyay D, Clements JC, Huntley JW, Kowalewski M. **2019**. Predation in the marine fossil record: Studies, data, recognition, environmental factors, and behavior. *Earth-Science Reviews* **194**: 472–520.

Knell RJ, Fortey RA. **2005**. Trilobite spines and beetle horns: sexual selection in the Palaeozoic? *Biology Letters* **1 (2)**: 196–199.

Knell RJ, Naish D, Tomkins JL, Hone DW. **2013**. Sexual selection in prehistoric animals: detection and implications. *Trends in Ecology & Evolution* **28 (1)**: 38–47.

Krynen JP, Sherwin L, Clarke I. **1990**. Stratigraphy and structure. In *Geological setting of gold and copper deposits in the Parkes area, New South Wales*. *Records of the Geological Survey of New South Wales* **23**: 1–76.

Lane PD. **1971**. *British Cheiruridae (Trilobita)*. London: Palaeontographical Society Monographs.

Lee JG, Choi DK, Pratt BR. **2001**. A teratological pygidium of the Upper Cambrian trilobite *Eugonocare* (*Pseudeugonocare*) *bispinatum* from the Machari Formation, Korea. *Journal of Paleontology* **75 (1)**: 216–218.

Leung TLF. **2017**. Fossils of parasites: what can the fossil record tell us about the evolution of parasitism? *Biological Reviews* **92 (1)**: 410–430.

Lindström G. **1885**. Förteckning på Gotlands siluriska crustacéer. *Öfversigt af Kongliga Vetenskaps-Akademiens Förhandlingar* **42 (3)**: 37–100, pls 112–116.

Lochman C. **1941**. A pathologic pygidium from the Upper Cambrian of Missouri. *Journal of Paleontology* **15 (3)**: 324–325.

Mitov PG, Dunlop JA, Bartel C. **2021**. A case of pedipalpal regeneration in a fossil harvestman (Arachnida: Opiliones). *Arachnologische Mitteilungen* **61 (1)**: 65–69.

Owen AW. **1983**. Abnormal cephalic fringes in the Trinucleidae and Harpetidae (Trilobita). *Special Papers in Paleontology* **30**: 241–247.

Owen AW. **1985**. Trilobite abnormalities. *Transactions of the Royal Society of Edinburgh: Earth Sciences* **76 (2-3)**: 255–272.

Pates S, Bicknell RDC, Daley AC, Zamora S. **2017**. Quantitative analysis of repaired and unrepaired damage to trilobites from the Cambrian (Stage 4, Drumian) Iberian Chains, NE Spain. *Palaios* **32 (12)**: 750–761.

Pates S, Bicknell RDC. **2019**. Elongated thoracic spines as potential predatory deterrents in olenelline trilobites from the lower Cambrian of Nevada. *Palaeogeography, Palaeoclimatology, Palaeoecology* **516 (2019)**: 295–306.

Percival IG, Glen RA. **2007**. Ordovician to earliest Silurian history of the Macquarie Arc, Lachlan Orogen, New South Wales. *Australian Journal of Earth Sciences* **54 (2-3)**: 143–165.

Pocock KJ. **1974**. A unique case of teratology in trilobite segmentation. *Lethaia* **7 (1)**: 63–66.

Přibyl A, Vaněk J. **1962**. Trilobitová fauna českého svrchního siluru (budňanu a lochkovu) a její biostratigrafický význam. *Sbornik Národniho Muzea v Praze Řada B, Přírodní vědy* **18 (2)**: 25–46.

Přibyl A, Vaněk J. **1973**. Zur Taxonomie und Biostratigraphie der crotalocephaliden Trilobiten aus dem böhmischen Silur und Devon. *Sbornik Narodniho muzea v Praze Rada C, Literarni historie* **28**: 37–92.

Přibyl A, Vaněk J. **1986**. A study of morphology and phylogeny of the family Harpetidae Hawle and Corda, 1847 (Trilobita). *Sbornik Národniho Muzea v Praze Řada B, Přírodní vědy* **42**: 1–72.

Ramsköld L. **1983**. Silurian cheirurid trilobites from Gotland. *Palaeontology* **26 (1)**: 175–210.

Ramsköld L. **1984**. Silurian odontopleurid trilobites from Gotland. *Palaeontology* **27 (2)**: 239–264.

Ramsköld L, Adrain JM, Edgecombe GD, Siveter DJ. **1994**. Silurian calymenid trilobite *Alcymene* n. gen., with new species from the Ludlow of Gotland, Sweden. *Journal of Paleontology* **68 (3)**: 556–569.

Rickards RB, Wright AJ, Thomas G. **2009**. Late Llandovery (early Silurian) dendroid graptolites from the cotton formation near Forbes, New South Wales. *Proceedings of the Linnean Society of New South Wales* **130:** 63–76.

Rudkin DM. **1979**. Healed injuries in *Ogygopsis klotzi* (Trilobita) from the Middle Cambrian of British Columbia. *Royal Ontario Museum, Life Sciences Occasional Paper* **32**: 1–8.

Rudkin DM. **1985**. Exoskeletal abnormalities in four trilobites. *Canadian Journal of Earth Sciences* **22 (3)**: 479–483.

Schneider CA, Rasband WS, Eliceiri KW. **2012**. NIH Image to ImageJ: 25 years of image analysis. *Nature Methods* **9 (7)**: 671–675.

Schrank E. **1969**. Odontopleuriden (Trilobita) aus silurischen Geschieben. *Berichte der Deutschen Geologischen Gesselschaft für Geologische Wissenschaften, Reihe A: Geologie und Paläontologie* **14**: 705–726.

Sherwin L. **1970**. Age of the Billabong Creek Limestone. *Quarterly Notes of the Geological Survey of New South Wales* **1**: 1–3.

Sherwin L. **1973**. Stratigraphy of the Forbes-Bogan Gate district. *Records of the Geological Survey of New South Wales* **15 (1)**: 47–101.

Sherwin L. **1974**. Llandovery graptolites from the Forbes District, New South Wales. Graptolite studies in honour of O. M. B. Bulman. *Special Papers in Palaeontology* **13**: 149–175.

Šnajdr M. **1976**. New proetid trilobites from the Silurian and Devonian of the Barrandian (Czechoslovakia). *Časopis pro Mineralogii a Geologii* **21**: 313–318.

Šnajdr M. **1978a**. Anomalous carapaces of Bohemian paradoxid trilobites. *Sborník Geologických Věd Paleontologie* **20**: 7–31.

Šnajdr M. **1978b**. Pathological neoplasms in the fringe of *Bohemoharpes* (Trilobita). *Věstník Ústředního Ústavu Geologického* **53**: 49–50.

Šnajdr M. **1979**. Note on the regenerative ability of injured trilobites. *Věstník Ústředniho ústavu geologického* **54 (3)**: 171–173, pls 171–172.

Šnajdr M. **1980**. Bohemian Silurian and Devonian Proetidae (Trilobita). *Rozpravy Ustředního ústavu geologického* **45**: 1–323, pls 321–364.

Šnajdr M. **1981a**. Bohemian Proetidae with malformed exoskeletons (Trilobita). *Sborník Geologických Věd Paleontologie* **24**: 37–61.

Šnajdr M. **1981b**. Ontogeny of some representatives of the trilobite genus *Scharyia*. *Sborník geologickćh věd Paleontologie* **24**: 7–35.

Šnajdr M. **1990**. *Bohemian trilobites*. Prague: Geological Survey Prague.

Strusz DL. **1980**. The Encrinuridae and related trilobite families, with a description of Silurian species from southeastern Australia. *Palaeontographica Abteilung A* **168**: 1–68.

Whiteley TE, Kloc GJ, Brett CE. **2002**. *Trilobites of New York: An Illustrated Guide*: Cornell University Press Ithaca, NY.

Whittington HB, Campbell KSW. **1967**. Silicified Silurian trilobites from Maine. *Bulletin of the Museum of Comparative Zoology* **135 (9)**: 447–483.

Zong R-W, Liu Q, Wei F, Gong Y-M. **2017**. Fentou Biota: a Llandovery (Silurian) shallow-water exceptionally preserved biota from Wuhan, central China. *The Journal of Geology* **125 (4)**: 469–478.

Zong R-W. **2021**. Abnormalities in early Paleozoic trilobites from central and eastern China. *Palaeoworld* **30**: 430–439.

398 **Figure captions**

399 **Figure 1:** Geological, stratigraphic, and geographical information for specimen locations. (A)
400 Map of Australia showing specimen location (red star) in New South Wales. (B) Geological map
401 showing rocks proximal to Forbes. Red stars indicate specimen location. (C) Panoramic view of
402 located where specimens were collected–Cotton Hill Quarry.

403 **Figure 2**: Reconstruction of *Odontopleura* (*Sinespinaspis*) *markhami* showing measurements
404 taken for analysed dataset. Abbreviations: cl: cranidial length, gw: glabellar width, tpl: combined
405 thorax and pygidium length.

406 **Figure 3:** *Odontopleura* (*Sinespinaspis*) *markhami* with additional and abnormal spine bases on
407 the right thoracic lobe. (A, B) AM F126904. (A) Complete specimen. (B) Close up of box in (A)
408 showing additional spine base on the seventh thoracic segment (white arrow). (C, D) AM
409 F118762. (C) Complete specimen. (D) Close up of box in (C) showing offset spine base (white
410 arrow) and additional spine base (black arrow).

411 **Figure 4:** *Odontopleura* (*Sinespinaspis*) *markhami* showing additional spine bases. (A, B) AM
412 F115089. (A) Complete specimen. (B) Close up of box in (A) showing additional spine bases on
413 first, third, and fourth thoracic segments on the right pleural lobe (white arrows). (C, D) AM
414 F115081. (C) Complete specimen. (D) Close up of box in (C) showing additional spine base on
415 the third thoracic segment of the left pleural lobe (white arrow). (E, F) AM F145135. (E)
416 Complete specimen. (F) Close up of box in (E) showing additional spine bases on second
417 thoracic segment on the right pleural lobe (white arrow).

418 **Figure 5:** *Odontopleura* (*Sinespinaspis*) *markhami* with additional and offset spine bases. (A, B)
419 AM F118772. (A) Complete specimen. (B) Close up of box in (A) showing offset spine on the

sixth thoracic segment of the right pleural lobe (white arrow). (C, D) AM F133034. (C) Complete specimen. (D) Close up of box in (C) showing additional spine bases on the sixth and eighth thoracic segments of the left pleural lobe (white arrows).

Figure 6: Natural log normalised bivariate plots of *Odontopleura* (*Sinespinaspis*) *markhami* of abnormal and standard specimens. Most abnormal specimens fall in the cluster of the second to largest specimens.

Supplemental Information 1: Measurement data from *Odontopleura* (*Sinespinaspis*) *markhami* examined in Figure 6.

Table 1(on next page)

Table 1: Record of abnormal Silurian trilobites.

Ordered by stage and the genus.

Taxon	Family	Epoch	Stage	Formation, country	Abnormality location	Abnormality description	Side	Citation and figure
Acernaspis elliptifrons (Esmark, 1833)	Lichidae	Llandovery	Aeronian	Solvik Formation, Sweden	Pygidium	Asymmetrically developed furrows	Both	Owen (1985, fig. 5t)
Encrinurus squarrosus Howells, 1982	Encrinuridae	Llandovery	Aeronian	Newlands Formation, Scotland	Pygidium	Damaged rib	Right	Howells (1982, pl. 8, fig. 12)
Encrinurus squarrosus	Encrinuridae	Llandovery	Aeronian	Newlands Formation, Scotland	Pygidium	Bifurcating rib	Right	Howells (1982, pl. 8, fig. 13)
Coronocephalus sp.	Encrinuridae	Llandovery	Telychian	Fentou Formation, China	Pygidium	Deformed, fused pygidial ribs	Right	Zong (2021, fig. 4D, E)
Coronocephalus sp.	Encrinuridae	Llandovery	Telychian	Fentou Formation, China	Pygidium	Truncated pygidial ribs	Right	Zong et al. (2017, fig. 3q); Zong (2021, fig. 4F, G)
Coronocephalus sp.	Encrinuridae	Llandovery	Telychian	Fentou Formation, China	Pygidium	Additional pygidial rib	Right	Zong (2021, fig. 4H, I)
Kailia intersulcata Chang, 1974	Encrinuridae	Llandovery	Telychian	Fentou Formation, China	Thorax	Thoracic spines 2–5 truncated, U-shaped indentation	Right	Zong (2021, fig. 4A–C)
Odontopleura (*Sinespinaspis*) *markhami*	Odontopleuridae	Llandovery	Telychian	Cotton Formation, NSW, Australia	Thorax	Additional thoracic spine base	Right	This article, Fig. 3A, B
Odontopleura (*Sinespinaspis*) *markhami*	Odontopleuridae	Llandovery	Telychian	Cotton Formation, NSW, Australia	Thorax	Additional spine base and offset spine base	Right	This article, Fig. 3C, D
Odontopleura (*Sinespinaspis*) *markhami*	Odontopleuridae	Llandovery	Telychian	Cotton Formation, NSW, Australia	Thorax	Additional posterior pleural band spine bases	Right	This article, Fig. 4A, B
Odontopleura (*Sinespinaspis*) *markhami*	Odontopleuridae	Llandovery	Telychian	Cotton Formation, NSW, Australia	Thorax	Additional thoracic spine base	Right	This article, Fig. 4C, D
Odontopleura (*Sinespinaspis*) *markhami*	Odontopleuridae	Llandovery	Telychian	Cotton Formation, NSW, Australia	Thorax	Additional thoracic spine base	Right	This article, Fig. 4E, F
Odontopleura (*Sinespinaspis*) *markhami*	Odontopleuridae	Llandovery	Telychian	Cotton Formation, NSW, Australia	Thorax	Additional thoracic spine base	Right	This article, Fig. 5A, B
Odontopleura (*Sinespinaspis) markhami*	Odontopleuridae	Llandovery	Telychian	Cotton Formation, NSW, Australia	Thorax	Additional posterior pleural band spine bases	Left	This article, Fig. 5C, D
Decoroproetus corycoeus (Conrad, 1842)	Proetidae	Wenlock	Sheinwoodian-Homerian	St. Clair Formation, Arkansas, USA	Thorax, pygidium	Thoracic segment 11? fused to	Right	Holloway (1980, pl. 3, fig. 4)

						pygidium		
Calymene frontosa Lindström, 1885	Calymenidae	Wenlock	?Sheinwoodian	Visby Beds, Sweden	Cephalon	Abnormal development of suture	Left	Owen (1985, fig. 5c)
Arctinurus boltoni (Bigsby, 1825)	Lichidae	Wenlock	Sheinwoodian	Rochester Formation, New York, USA	Pygidium	Truncated posteriormost pygidial spine, 'W'-shaped injury	Right	Rudkin (1985, fig. 1A, B)
Arctinurus boltoni	Lichidae	Wenlock	Sheinwoodian	Rochester Formation, New York, USA	Thorax, pygidium	Large 'U'-shaped indentation, posterior thorax, extending onto pygidium	Right	Babcock (1993b, p. 36, no figure number)
Arctinurus boltoni	Lichidae	Wenlock	Sheinwoodian	Rochester Formation, New York, USA	Cephalon, thorax, pygidium	'U'-shaped indentation, cephalon; 'V'-shaped indentation thoracic segments 3–4; 'W'-shaped indentation thoracic segments 8–10 'U'-shaped indentation pygidium	Left (cephlaon, thorax) Right (pygidium)	Whiteley et al. (2002 fig. 2.9B); Chinnici & Smith (2015, fig. 434)
Arctinurus boltoni	Lichidae	Wenlock	Sheinwoodian	Rochester Formation, New York, USA	Thorax, pygidium	Thoracic spines 1–4 truncated, 'U'-shaped indentation, truncated pygidial spines	Right (thorax) Left (pygidium)	Chinnici & Smith (2015, fig. 432)
Arctinurus boltoni	Lichidae	Wenlock	Sheinwoodian	Rochester Formation, New York, USA	Cephalon, thorax	'U'-shaped indentation, posterior cephalon, single segment injury, 4th thoracic segment	Right	Chinnici & Smith (2015, fig. 433)
Arctinurus boltoni	Lichidae	Wenlock	Sheinwoodian	Rochester Formation, New York, USA	Pygidium	Abnormal pygidial spine	Left	Bicknell et al. (2019, fig. 3A, B)

Arctinurus boltoni	Lichidae	Wenlock	Sheinwoodian	Rochester Formation, New York, USA	Pygidium	Reduced pygidial spine	Right	Bicknell et al. (2019, fig. 3C, D)
Arctinurus boltoni	Lichidae	Wenlock	Sheinwoodian	Rochester Formation, New York, USA	Pygidium	'U'-shaped indentation	Right	Bicknell et al. (2019, fig. 3E, F)
Arctinurus boltoni	Lichidae	Wenlock	Sheinwoodian	Rochester Formation, New York, USA	Pygidium	Rounded pygidial spine	Right	Bicknell et al. (2019, fig. 4A, B)
Arctinurus boltoni	Lichidae	Wenlock	Sheinwoodian	Rochester Formation, New York, USA	Pygidium	'W'-shaped indentation	Right	Bicknell et al. (2019, fig. 4C, D)
Arctinurus boltoni	Lichidae	Wenlock	Sheinwoodian	Rochester Formation, New York, USA	Pygidium	'W'-shaped indentation	Right	Bicknell et al. (2019, fig. 4E, F)
Arctinurus boltoni	Lichidae	Wenlock	Sheinwoodian	Rochester Formation, New York, USA	Thorax	Single segment injury, thoracic segment 2	Right	Bicknell et al. (2019, fig. 5A, B)
Arctinurus boltoni	Lichidae	Wenlock	Sheinwoodian	Rochester Formation, New York, USA	Thorax and pygidium	Two 'V'-shaped indentations (Thoracic segments 1–2; thoracic segments 7–8); pygidium slightly truncated	Right	Bicknell et al. (2019, fig. 6A, B)
Calymene niagarensis Hall, 1843	Calymenidae	Wenlock	Sheinwoodian	Rochester Formation, New York, USA	Thorax	'L'-shaped indentation, thoracic segments 1–4	Right	Chinnici & Smith (2015, fig. 432)
Calymene sp.	Calymenidae	Wenlock	Sheinwoodian	Rochester Formation, New York, USA	Cephalon	Borings on genal spine	Left	Whiteley et al. (2002, fig. 2.15D–F)
Coronocephalus urbis Strusz, 1980	Encrinuridae	Wenlock	Sheinwoodian	Walker Volcanics, Australian Central Territory, Australia	Pygidium	Bifurcated rib	Right	Strusz (1980, pl. 1, fig. 17)
Dalmanites limulurus (Green, 1832)	Dalmanitidae	Wenlock	Sheinwoodian	Rochester Formation, New York, USA	Thorax	'U'-shaped indentation, thoracic segments 2–5	Right	Chinnici & Smith (2015, fig. 437)
Dalmanites limulurus	Dalmanitidae	Wenlock	Sheinwoodian	Rochester Formation, New York, USA	Thorax	U'-shaped indentation, thoracic segments 1–3	Right	Chinnici & Smith (2015, fig. 438)

Dalmanites limulurus	Dalmanitidae	Wenlock	Sheinwoodian	Rochester Formation, New York, USA	Thorax	'U'-shaped indentations, thoracic segments 2–4 and 8–1	Left	Chinnici & Smith (2015, fig. 439); Whiteley et al. (2002, fig. 2.15A)
Dalmanites limulurus	Dalmanitidae	Wenlock	Sheinwoodian	Rochester Formation, New York, USA	Thorax, pygidium	U'-shaped indentation, thoracic segments 10–11 extending into pygidium	Left	Chinnici & Smith (2015, fig. 440)
Dalmanites limulurus	Dalmanitidae	Wenlock	Sheinwoodian	Rochester Formation, New York, USA	Thorax	U'-shaped indentation, thoracic segments 5–11	Left	Chinnici & Smith (2015, fig. 441)
Dalmanites limulurus	Dalmanitidae	Wenlock	Sheinwoodian	Rochester Formation, New York, USA	Pygidium	Terminal, medial spine missing	Midline	Whiteley et al. (2002, fig. 2.15C)
Japonoscutellum sp.	Encrinuridae	Wenlock	Sheinwoodian	Yarralumla Formation, New South Wales, Australia	Pygidium	Bifurcating axial rib	Right	Bicknell & Smith (2021, fig. 3b, c)
Exallaspis bufo (Ramsköld, 1984)	Odontopleuridae	Wenlock	Homerian	Mulde Beds, Sweden	Cranidium	Asymmetrical crandium	Left	Ramsköld (1984, pl. 31, fig. 1)
Exallaspis bufo	Odontopleuridae	Wenlock	Homerian	Mulde Beds, Sweden	Pygidium	Additional terminal spine	Midline	Ramsköld (1984, pl. 31, fig. 5)
Interproetus truncus Šnajdr, 1980	Proetidae	Wenlock	Homerian	Liten Formation, Czech Republic	Thorax	Reduced and fused pleurae	Right	Šnajdr (1980, pl. XLVIII, figs 1, 2)
Ktenoura retrospinosa Lane, 1971	Cheiruridae	Wenlock	Homerian	Much Wenlock Limestone Formation, England	Pygidium	Reduced spine	Right	Lane (1971, pl. 6, fig. 9a, b)
Odontopleura ovata Emmrich, 1839	Odontopleuridae	Wenlock	Homerian	Liten Formation, Czech Republic	Thorax	'U'-shaped indentation, thoracic segments 4–8	Right	Šnajdr (1979, pl. 1)
Exallaspis mutica (Emmrich, 1844)	Odontopleuridae	Wenlock–Ludlow	—	Grünlich-Graues Graptolithengestein, Germany	Pygidium	Single spine injury	Left	Schrank (1969, pl. IV, fig. 7)
Odontopleura ovata	Odontopleuridae	Wenlock–Ludlow	—	Grünlich-Graues Graptolithengestein, Germany	Pygidium	Asymmetric medial lobe	Left	Schrank (1969, pl II, fig. 4)
Alcymene lindstroemi	Calymenidae	Ludlow	Gorstian	Hemse Marl, Sweden	Cephalon	Overdeveloped glabellar region	Midline	Ramsköld et al. (1994, fig. 5, 9)

Ramsköld et al., 1994								
Bohemoharpes ungula viator Přibyl & Vaněk, 1986	Harpetidae	Ludlow	Gorstian	Kopanina Formation, Czech Republic	Cephalon	Asymmetrical cranidial region	Right larger than left	Přibyl & Vaněk (1986, pl. 2, fig.1)
Bohemoharpes ungula	Harpetidae	Ludlow	Gorstian	Kopanina Formation, Czech Republic	Cephalon	Multiple neoplasms	Left	Šnajdr (1978a, pl. I, figs. 1–5)
Bohemoharpes ungula	Harpetidae	Ludlow	Gorstian	Kopanina Formation, Czech Republic	Cephalon	Neoplasms on genal spine	Left	Šnajdr (1978a, pl. I, figs. 6, 7); Šnajdr (1990, p. 63)
Prionopeltis archiaci (Barrande, 1846)	Proetidae	Ludlow	Gorstian	Kopanina Formation, Czech Republic	Pygidium	Single spine injury	Right	Šnajdr (1981a, pl. I, fig. 1)
Prionopeltis archiaci	Proetidae	Ludlow	Gorstian	Kopanina Formation, Czech Republic	Pygidium	'U'-shaped indentation	Right	Šnajdr (1981a, pl. II, fig. 2)
Prionopeltis archiaci	Proetidae	Ludlow	Gorstian	Kopanina Formation, Czech Republic	Pygidium	Fused pygidial ribs, 'W'-shaped indentation	Right	Šnajdr (1981a, pl V, fig. 4)
Prionopeltis archiaci	Proetidae	Ludlow	Gorstian	Kopanina Formation, Czech Republic	Pygidium	Pinched pygidial ribs	Left	Šnajdr (1981a, pl V, fig. 5; pl VIII, fig. 3)
Prionopeltis archiaci	Proetidae	Ludlow	Gorstian	Kopanina Formation, Czech Republic	Pygidium	Additional terminal spine	Midline	Šnajdr (1981a, pl VII, fig. 6)
Prionopeltis archiaci	Proetidae	Ludlow	Gorstian	Kopanina Formation, Czech Republic	Pygidium	Thin terminal spines	Midline	Šnajdr (1981a, pl VIII, fig. 4)
Prionopeltis archiaci	Proetidae	Ludlow	Gorstian	Kopanina Formation, Czech Republic	Pygidium	Ribs poorly developed	Right	Šnajdr (1981a, pl VIII, fig. 5)
Prionopeltis archiaci	Proetidae	Ludlow	Gorstian	Kopanina Formation, Czech Republic	Pygidium	Additional spine	midline	Šnajdr (1981a, pl VIII, fig. 6)
Prionopeltis archiaci	Proetidae	Ludlow	Gorstian	Kopanina Formation, Czech Republic	Pygidium	Additional spine	Left	Šnajdr (1981a, pl VIII, fig. 7)
Prionopeltis archiaci	Proetidae	Ludlow	Gorstian	Kopanina Formation, Czech Republic	Pygidium	Additional spine	Midline	Šnajdr (1981a, pl VIII, fig. 8)
Prionopeltis dracula Šnajdr,	Proetidae	Ludlow	Gorstian	Kopanina Formation, Czech	Pygidium	Additional spines	Both	Šnajdr (1980, not figured)

1980				Republic				
Scharyia micropyga (Hawle & Corda, 1847)	Aulacopleuridae	Ludlow	Gorstian	Kopanina Formation, Czech Republic	Pygidium	'U'-shaped indentation, spine abnormally developed	Right	Šnajdr (1981a, pl IV, fig. 2)
Scharyia micropyga	Aulacopleuridae	Ludlow	Gorstian	Kopanina Formation, Czech Republic	Pygidium	Additional ribs	Midline	Šnajdr (1981b, pl. XI, fig. 1)
Scharyia micropyga	Aulacopleuridae	Ludlow	Gorstian	Kopanina Formation, Czech Republic	Pygidium	Abnormally developed interring furrows	Midline	Šnajdr (1981b, pl. XI, fig. 2)
Scharyia micropyga	Aulacopleuridae	Ludlow	Gorstian	Kopanina Formation, Czech Republic	Pygidium	Abnormally developed interring furrows	Midline	Šnajdr (1981b, pl. XI, fig. 3)
Scharyia micropyga	Aulacopleuridae	Ludlow	Gorstian	Kopanina Formation, Czech Republic	Pygidium	Abnormal axial ring	Midline	Šnajdr (1981b, pl. XI, fig. 4)
Scharyia micropyga	Aulacopleuridae	Ludlow	Gorstian	Kopanina Formation, Czech Republic	Pygidium	Abnormal axial ring	Midline	Šnajdr (1981b, pl. XI, fig. 7)
Scharyia micropyga	Aulacopleuridae	Ludlow	Gorstian	Kopanina Formation, Czech Republic	Pygidium	Poorly developed axial rings	Midline	Šnajdr (1981b, pl. XI, fig. 8)
Sphaerexochus latifrons Angelin, 1854	Cheiruridae	Ludlow	Gorstian	Hemse Marl, Sweden	Cephalon	Pathological development on free cheek	Right	Ramsköld (1983, pl. 19, fig. 6)
Kosovopeltis nebula Campbell, 1967	Scutelluidae	Ludlow	Gorstian–early Ludfordian	Henryhouse Formation, Oklahoma, USA	Thorax	Overdeveloped pleurae	Right	Campbell (1967, pl. 2 figs 5, 6)
Batocara robustus (Mitchell, 1924)	Encrinuridae	Ludlow	Ludfordian	Black Bog Shale, New South Wales	Thorax	Bifurcated pleural rib	Right	Strusz (1980, pl. 3, fig. 7)
Batocara robustus	Encrinuridae	Ludlow	Ludfordian	Black Bog Shale, New South Wales, Australia	Pygidium	Offset axial nodes	Midline	Bicknell & Smith (2021, fig. 2a, b)
Batocara robustus	Encrinuridae	Ludlow	Ludfordian	Black Bog Shale, New South Wales, Australia	Pygidium	Bifurcating axial rib	Left	Bicknell & Smith (2021), fig. 2c, f
Batocara robustus	Encrinuridae	Ludlow	Ludfordian	Black Bog Shale, New South Wales, Australia	Pygidium	Additional axial node	Midline	Bicknell & Smith (2021, fig. 2d e)
Didrepanon squarrosum	Cheiruridae	Ludlow	Ludfordian	Kopanina Formation, Czech Republic	Crandium	Asymmetric glabellar furrows	Left	Přibyl & Vaněk (1973, pl. I, fig. 1)

Leonaspis rattei (Etheridge & Mitchell, 1869)	Odontopleurinae	Ludlow	Ludfordian	Black Bog Shale, New South Wales, Australia	Thorax	Asymmetrical thoracic pleural nodes	Both	Bicknell & Smith (2021, fig. 3a)
Harpidella (*Rhinotarion*) *setosum* Whittington & Campbell, 1967	Aulacopleuridae	Ludlow	?Ludfordian	Hardwood Mountain Formation, Maine, USA	Cephalon	Asymmetrical cranidium	Left larger than right	Whittington & Campbell (1967, pl. 5, fig. 5, 6)
Prionopeltis striata (Barrande, 1846)	Proetidae	Pridoli	—	Přídolí Formation, Czech Republic	Pygidium	Single spine injury	Left	Šnajdr (1981a, pl. I, fig. 2)
Prionopeltis striata	Proetidae	Pridoli	—	Přídolí Formation, Czech Republic	Pygidium	'W'-shaped indentation	Left	Šnajdr (1981a, pl. I, fig. 3)
Prionopeltis striata	Proetidae	Pridoli	—	Přídolí Formation, Czech Republic	Pygidium	Spines removed	Left	Šnajdr (1981a, pl. II, fig. 3)
Prionopeltis striata	Proetidae	Pridoli	—	Přídolí Formation, Czech Republic	Pygidium	'V'-shaped indentation	Right	Šnajdr (1981a, pl. II, fig. 5)
Prionopeltis striata	Proetidae	Pridoli	—	Přídolí Formation, Czech Republic	Pygidium	Fused, deformed ribs	Left	Šnajdr (1981a, pl. III, fig. 1)
Prionopeltis striata	Proetidae	Pridoli	—	Přídolí Formation, Czech Republic	Pygidium	'V'-shaped indentation	Left	Šnajdr (1981a, pl. III, fig. 8)
Prionopeltis striata	Proetidae	Pridoli	—	Přídolí Formation, Czech Republic	Cephalon	Shallow 'U'-shaped indentation in free cheek	Right	Šnajdr (1981a, pl. IV, fig. 5)
Prionopeltis striata	Proetidae	Pridoli	—	Přídolí Formation, Czech Republic	Pygidium	Pathological growth	Midline	Šnajdr (1981a, pl. IV, fig. 6); De Baets et al. (2021, fig. 6.2f)
Prionopeltis striata	Proetidae	Pridoli	—	Přídolí Formation, Czech Republic	Pygidium	Additional spine, posteriormost section	Midline	Šnajdr (1981a, pl. VII, fig. 2)
Prionopeltis striata	Proetidae	Pridoli	—	Přídolí Formation, Czech Republic	Pygidium	'U'-shaped indentation	Midline	Šnajdr (1981a, pl. VII, fig. 4)
Prionopeltis striata	Proetidae	Pridoli	—	Přídolí Formation, Czech Republic	Pygidium	'U'-shaped indentation	Midline	Šnajdr (1981a, pl. VII, fig. 5)
Prionopeltis striata	Proetidae	Pridoli	—	Přídolí Formation, Czech Republic	Pygidium	'U'-shaped indentation	Midline	Šnajdr (1981a, pl. VIII, fig. 1)
Prionopeltis striata	Proetidae	Pridoli	—	Přídolí Formation, Czech Republic	Pygidium	'W'-shaped indentation	Left	Šnajdr (1981a, pl. VIII, fig. 2)
Scharyia nympha Chlupáč, 1971	Aulacopleuridae	Pridoli	—	Přídolí Formation, Czech Republic	Pygidium	Additional ribs, asymmetrically developed	Midline	Šnajdr (1981b, pl. XII, fig. 7)

Tetinia minuta (Přibyl & Vaněk, 1962)	Proetidae	Pridoli	—	Přídolí Formation, Czech Republic	Pygidium	Reduced ribs	Right	Šnajdr (1981a, pl. II, fig. 7)
Tetinia minuta	Proetidae	Pridoli	—	Přídolí Formation, Czech Republic	Pygidium	'U'-shaped indentation, pinched ribs	Right	Šnajdr (1981a, pl. II, fig. 8)
Tetinia minuta	Proetidae	Pridoli	—	Přídolí Formation, Czech Republic	Pygidium	U'-shaped indentation, abnormal ribs	Left	Šnajdr (1981a, pl. III, fig. 4)
Tetinia minuta	Proetidae	Pridoli	—	Přídolí Formation, Czech Republic	Pygidium	Asymmetrical pygidium, abnormal ribs	Left	Šnajdr (1981a, pl. III, fig. 5)
Tetinia minuta	Proetidae	Pridoli	—	Přídolí Formation, Czech Republic	Pygidium	Asymmetrical medial lobe, abnormal ribs	Left	Šnajdr (1981a, pl. III, fig. 6)

1 **Table 1: Record of abnormal Silurian trilobites. Ordered by stage and the genus.**

Figure 1

Figure 1: Geological, stratigraphic, and geographical information for specimen locations.

(A) Map of Australia showing specimen location (red star) in New South Wales. (B) Geological map showing rocks proximal to Forbes. Red stars indicate specimen location. (C) Panoramic view of located where specimens were collected–Cotton Hill Quarry.

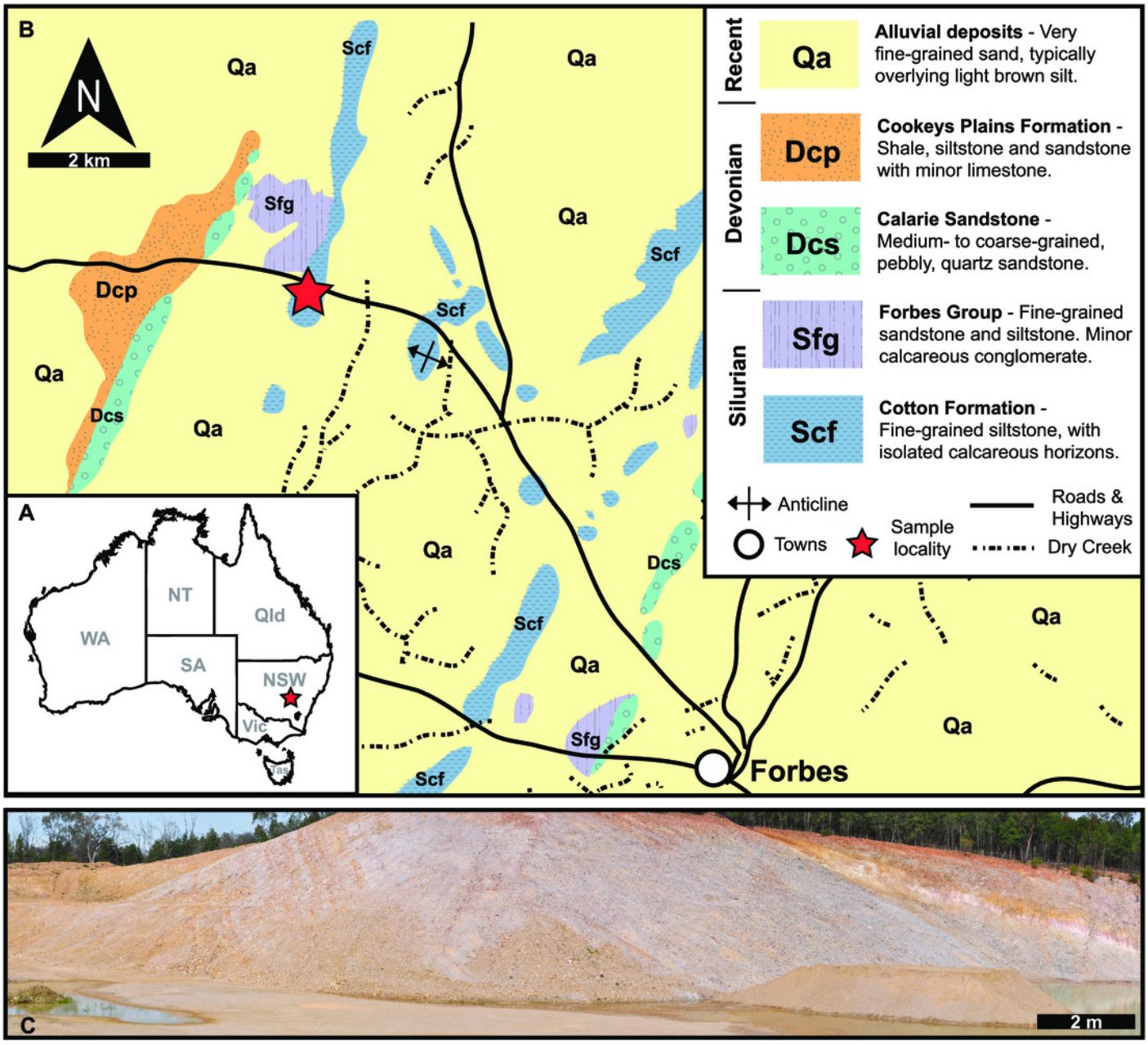

Figure 2

Figure 2: Reconstruction of *Odontopleura* (*Sinespinaspis*) *markhami* showing measurements taken for analysed dataset.

Abbreviations: cl: cranidial length, gw: glabellar width, tpl: combined thorax and pygidium length.

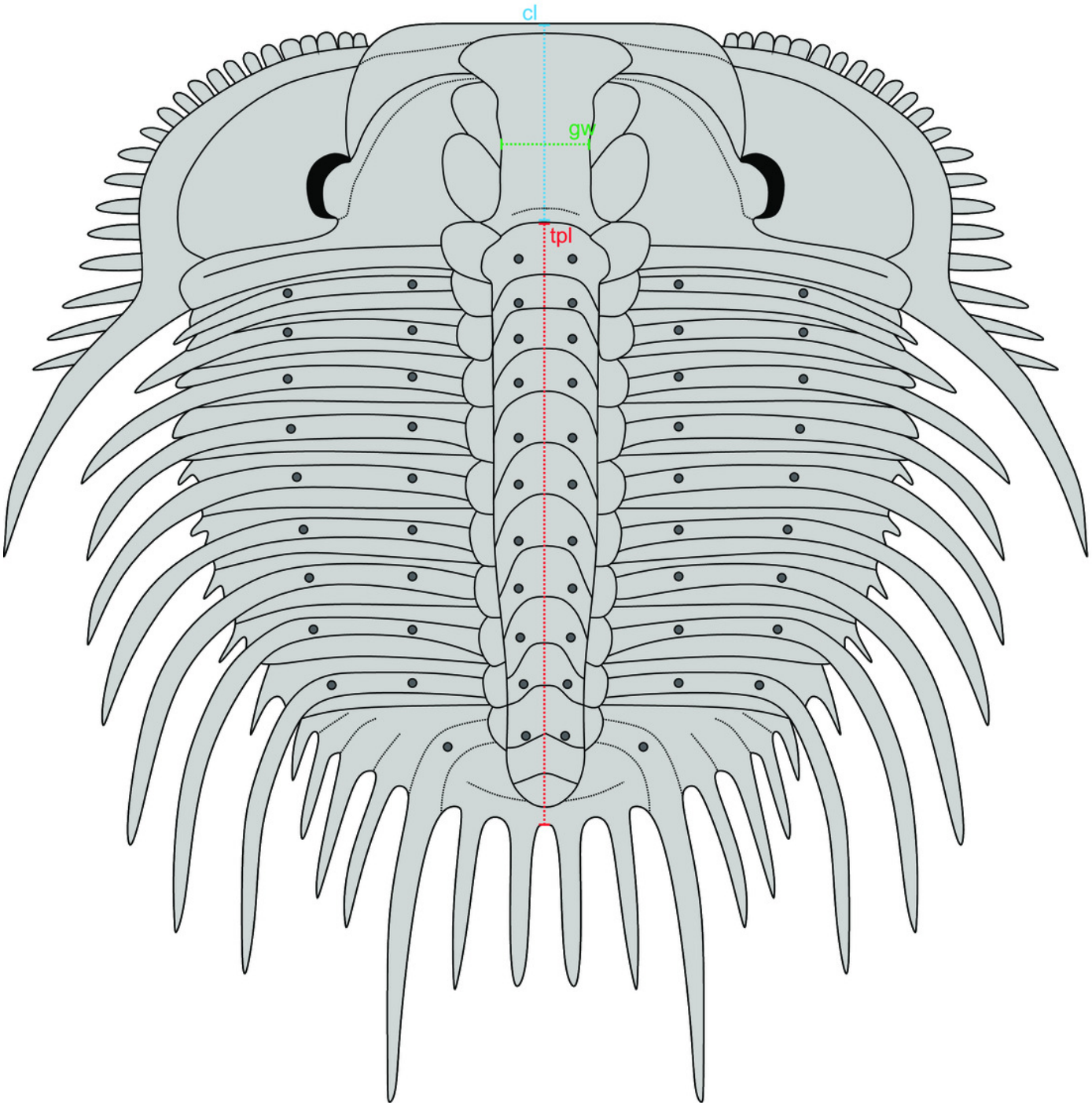
cl
gw
tpl

Figure 3

Figure 3: *Odontopleura* (*Sinespinaspis*) *markhami* with additional and abnormal spine bases on the right thoracic lobe.

(A, B) AM F126904. (A) Complete specimen. (B) Close up of box in (A) showing additional spine base on the seventh thoracic segment (white arrow). (C, D) AM F118762. (C) Complete specimen. (D) Close up of box in (C) showing offset spine base (white arrow) and additional spine base (black arrow).

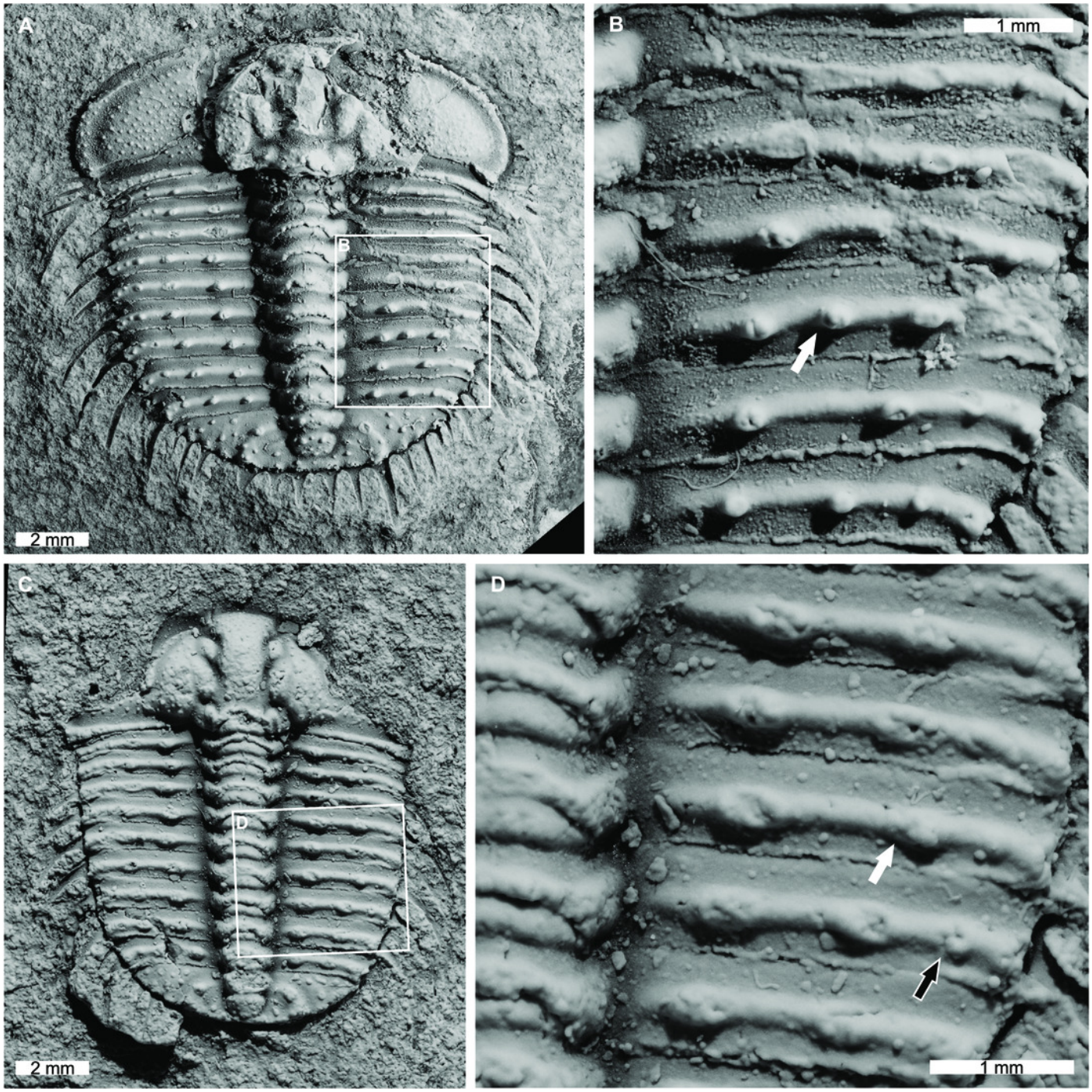
A
B
2 mm
B
1 mm
C
D
2 mm
D
1 mm

Figure 4

Figure 4: *Odontopleura* (*Sinespinaspis*) *markhami* showing additional spine bases.

(A, B) AM F115089. (A) Complete specimen. (B) Close up of box in (A) showing additional spine bases on first, third, and fourth thoracic segments on the right pleural lobe (white arrows). (C, D) AM F115081. (C) Complete specimen. (D) Close up of box in (C) showing additional spine base on the third thoracic segment of the left pleural lobe (white arrow). (E, F) AM F145135. (E) Complete specimen. (F) Close up of box in (E) showing additional spine bases on second thoracic segment on the right pleural lobe (white arrow).

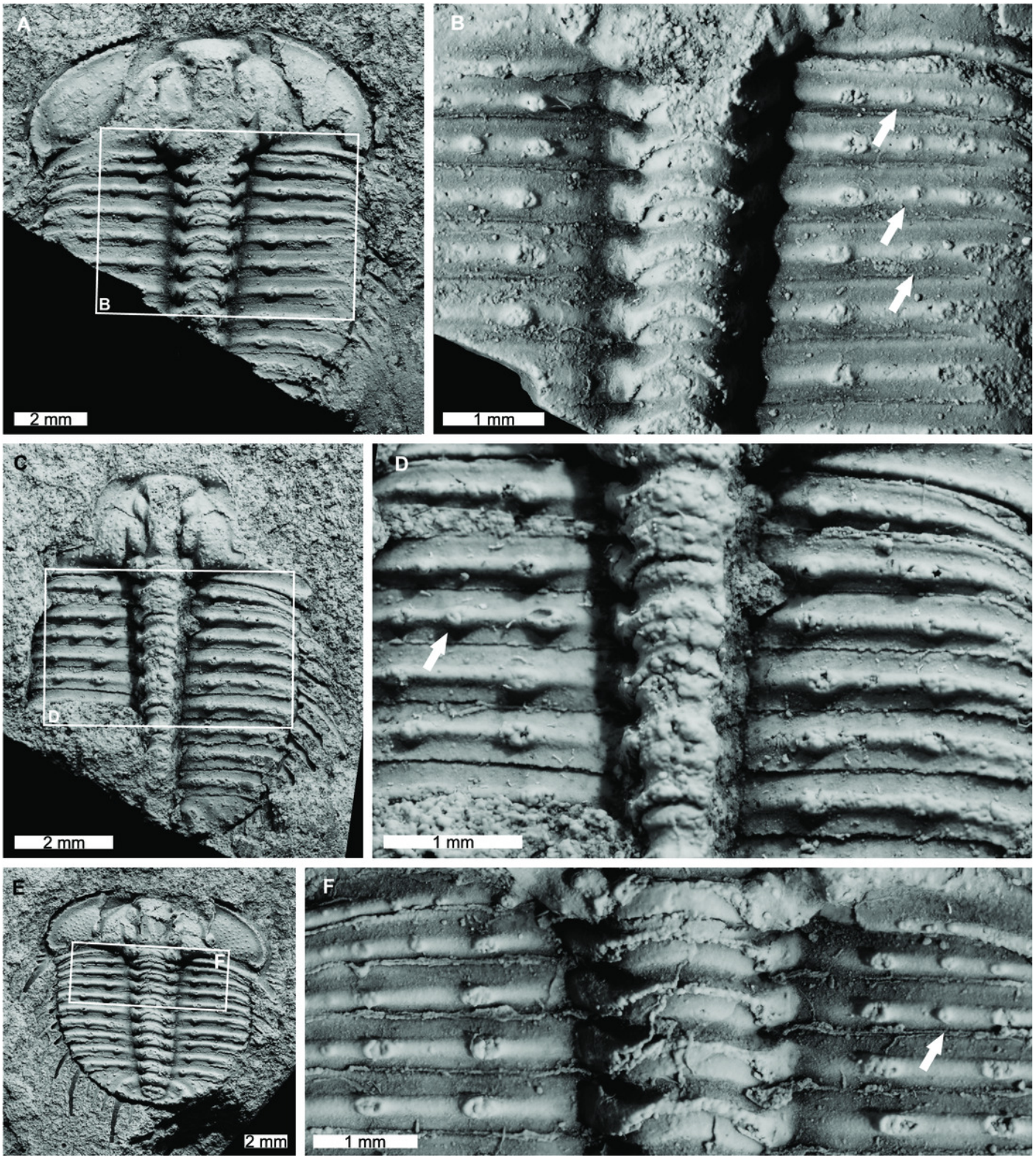
A
B
2 mm
B
1 mm
C
D
2 mm
D
1 mm
E
F
2 mm
F
1 mm

Figure 5

Figure 5: *Odontopleura* (*Sinespinaspis*) *markhami* with additional and offset spine bases.

(A, B) AM F118772. (A) Complete specimen. (B) Close up of box in (A) showing offset spine on the sixth thoracic segment of the right pleural lobe (white arrow). (C, D) AM F133034. (C) Complete specimen. (D) Close up of box in (C) showing additional spine bases on the sixth and eighth thoracic segments of the left pleural lobe (white arrows).

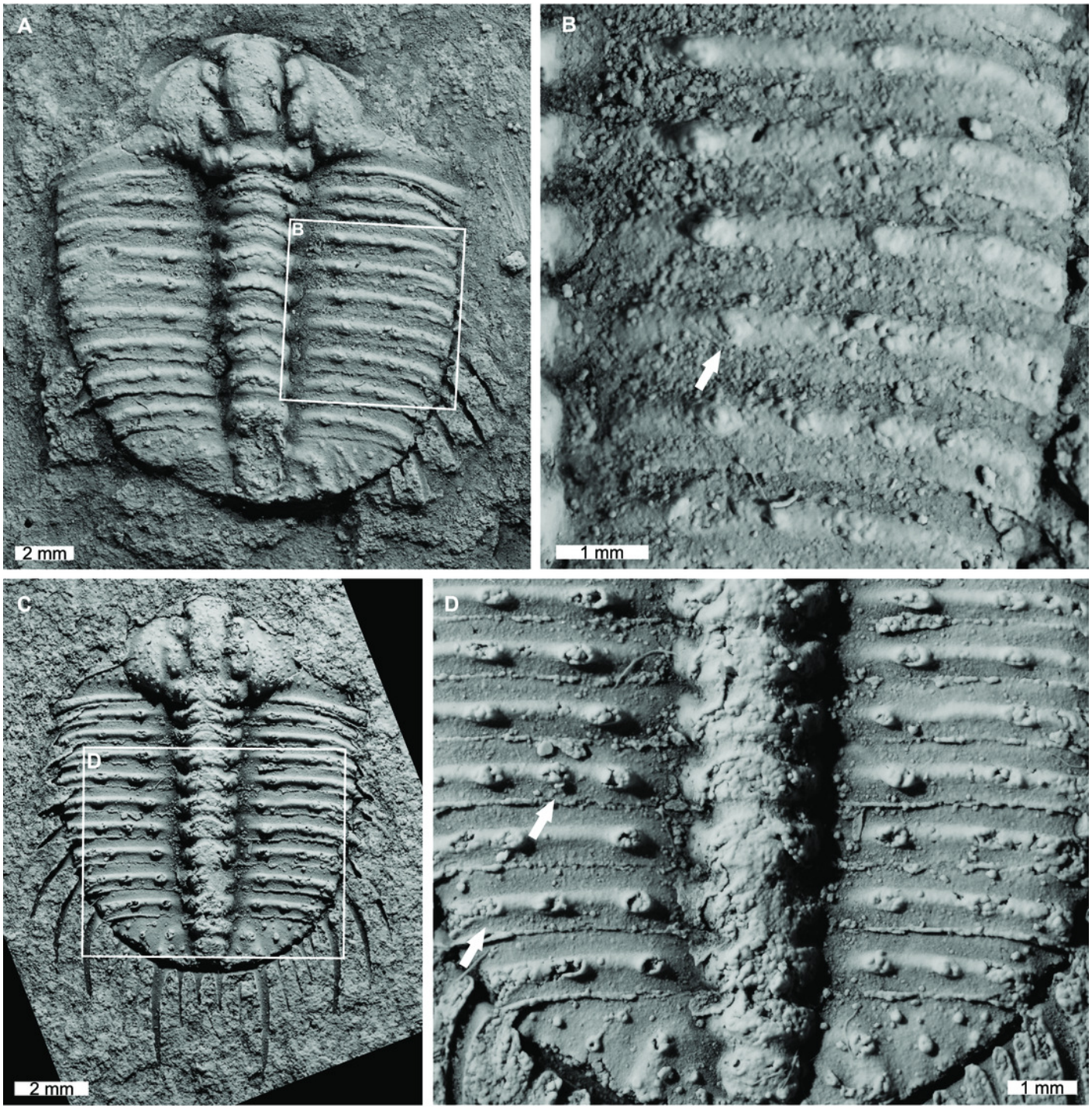
A
B
2 mm
B
1 mm
C
D
2 mm
D
1 mm

Figure 6

Figure 6: Natural log normalised bivariate plots of *Odontopleura* (*Sinespinaspis*) *markhami* of abnormal and standard specimens.

Most abnormal specimens fall in the cluster of the second to largest specimens.

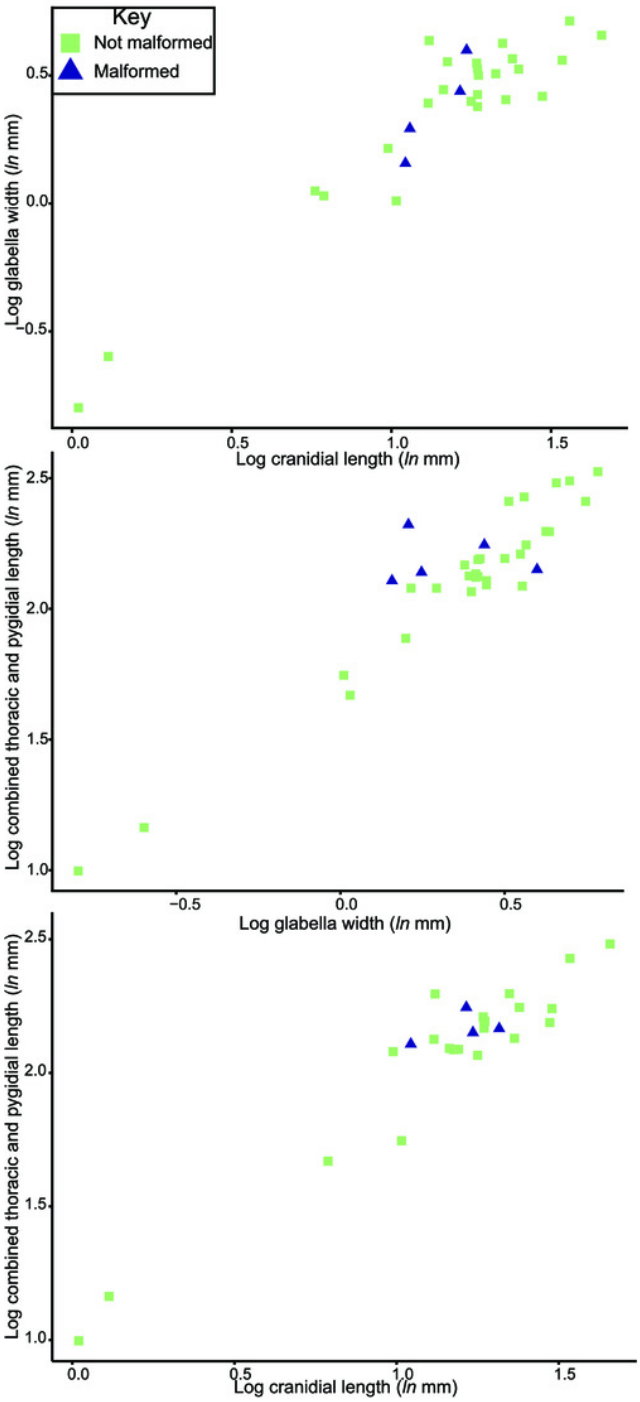
Key
Not malformed
Malformed
Log glabella width (ln mm)
Log cranidial length (ln mm)
Log combined thoracic and pygidial length (ln mm)
Log glabella width (ln mm)
Log combined thoracic and pygidial length (ln mm)
Log cranidial length (ln mm)